

Analysis of the Drying Kinetics of Freeze-Dried Persimmon at Different Cabin Pressures using Artificial Neural Network Method

Muhammed Emin Topal^{1*}, Birol Şahin¹ & Serkan Vela²

¹Faculty of Engineering and Architecture, Department of Mechanical Engineering, Recep Tayyip Erdogan University, 53100, Rize/Türkiye

²Electronics and Communication Engineering, Technology of Faculty, Karadeniz Technical University, 61830, Trabzon/Türkiye

Received 31 July 2024; revised 06 June 2025; accepted 18 June 2025

The main objective of this study is to freeze dry persimmon (*Diospyros kaki*) at three different cabin pressures (0.008 mbar, 0.010 mbar and 0.012 mbar) and product thicknesses (3 mm, 5 mm, and 7 mm) and, examine the drying kinetics, and assess the accuracy of artificial neural networks (ANN) in forecasting critical drying parameters, including Moisture Content (MC), Drying Rate (DR), and dimensionless Mass loss Ratio (MR). In this study, a feed forward ANN with a Multilayer Perceptron (MLP) architecture was designed to simulate and predict the freeze-drying behavior of persimmons. The ANN modeling, developed using MATLAB software while accounting for different product thicknesses and cabin pressures, demonstrated a test performance value of 0.99781 and an overall performance value of 0.99896. The drying time for persimmons ranged from 1080 minutes (3 mm, 0.008 mbar) to 2160 minutes (7 mm, 0.012 mbar). It was observed that reducing cabin pressure and product thickness resulted in decreased drying time. The highest drying rate (0.213%/min) was achieved with a 3 mm thick product at 0.008 mbar cabin pressure. Depending on the product thickness and cabin pressure, the Alibas model (3 mm, 0.008 mbar), the Improved Midilli-Kucuk model (3 mm, 0.010 mbar; 5 mm, 0.008 mbar; 5 mm, 0.012 mbar; and 7 mm, 0.010 mbar), and the Balbay & Sahin model (3 mm, 0.012 mbar; 5 mm, 0.010 mbar; 7 mm, 0.008 mbar; and 7 mm, 0.012 mbar) were found to be the most effective in describing the drying process of persimmons. These results suggest that ANNs are capable of effectively modeling the freeze-drying process of persimmons.

Keywords: Artificial neural network, Drying behavior, Drying kinetics, Freeze-drying, Persimmon

Introduction

The persimmon, which first originated in China and has spread over a vast geographical area from Asia to America, is a fruit that grows in subtropical climates.¹ Belonging to the Ebenaceae family, the persimmon has beneficial effects on human health, such as boosting the immune system, increasing resistance, and balancing blood pressure and cholesterol.² It is particularly preferred by consumers due to its richness in vitamins A and C and its unique pleasant taste and aroma. The persimmon can be consumed directly as a fruit and is also frequently processed into various products such as jam, marmalade, and ice cream.³

The high moisture content of persimmon leads to rapid spoilage of the product. Various methods are employed to prevent spoilage, preserve nutritional value, and extend shelf life and storage duration. Among these methods, drying stands out as a primary technique. Drying is a fundamental process

commonly used in the food industry to reduce the moisture content of products through various techniques.⁴ Drying can be carried out using different methods such as refractance window drying, microwave drying, spray drying, drum drying and freeze-drying (FD).^{5,6} Compared to other drying methods, the FD method stands out as a drying technique that minimizes losses in the product's unique properties and extends its shelf life under appropriate storage conditions. FD is a process where the ice crystals in the products transition directly to the gas phase under specific pressure and temperature conditions.⁷ A review of the literature shows that numerous products, such as orange⁸, grapefruit⁹, and strawberry¹⁰, have been subjected to FD, with their thin-layer drying kinetics thoroughly assessed.

In recent years, Artificial Neural Networks (ANNs) have emerged as a crucial method for modeling complex relationships across nearly all industrial sectors. In the food drying industry, ANNs have started to be widely used to enhance product quality and save time and costs. A model capable of

* Author for Correspondence

E-mail: muhammedemin.topal@erdogan.edu.tr

accurately predicting the drying process using the predictive power of ANNs, based on input variables such as Product Thickness (PT), Cabin Pressure (CP), and Drying Time (DT), is of critical importance for time and energy savings. Literature reviews indicate that various products and drying methods, including linden leaves¹¹, onion puree¹², *Citrus medica*¹³, lucuma powder¹⁴, and Tahiti lemon¹⁵ have been subjected to ANN analysis. Azadbakht *et al.* (2017)⁽¹⁶⁾ conducted a study on drying potato cubes at different temperatures, air velocities, and bed depths. They used ANNs to predict energy and exergy parameters, finding R² values ranging from 0.98394 to 0.99843, demonstrating the potential use of ANNs in intelligent drying processes. Omari *et al.* (2018)⁽¹⁷⁾ conducted mushroom drying experiments using microwave-hot air-drying methods. They employed a feedforward multilayer perceptron (MLP) ANN to predict the variation in moisture content of the product over time. The results indicated R² values ranging from 0.9801 to 0.9895 and RMSE values between 0.3503 and 0.3996, demonstrating that ANNs are effective tools for characterizing the mushroom drying process.

In the food drying industry, parameters such as time, energy consumption, and total cost are crucial, similar to other sectors. Moreover, preserving specific qualities of dried food, including color, taste, and shape, is vital for consumer preference. In this study, unlike the literature, persimmons with different thicknesses were freeze-dried under different cabin pressures, and drying kinetic curves were estimated with artificial neural networks. This study selected FD to dry persimmons, as it minimizes quality losses. Data collected during the FD process were applied to different thin-layer models and ANNs described in the literature. Additionally, comparisons were made between traditional mathematical modeling and ANNs, which offer superior learning capacity and greater flexibility.

Materials and Methods

Material

The persimmons used in the experimental study were harvested in November 2023 in the Rize province of Türkiye (41.01450° N, 40.53251° E). Prior to the experimental drying process, the fruits were washed, cleaned, and then sliced to PT of 3 mm, 5 mm, and 7 mm. They were subsequently frozen at -40°C for 24 hours. In order to ascertain the moisture content of the persimmons, a 20-gram sample was

placed in a drying chamber (Jeio-21E, Jeio Tech Company, Korea) set at 105°C, and the mass loss change was measured after 24 hours. The measurements revealed that the moisture content of the persimmons was 80.0 ± 0.2%.

Methods

Freeze-drying Methodology

The persimmons, which had been sliced into different PTs and frozen, were placed on the trays of a FD device (Free Zone 2.5 Manual, Labconco Company, USA) and subjected to the drying process under three different CPs (0.008 mbar, 0.010 mbar, and 0.012 mbar). During the experiments, a precision balance (EGY-50, Dikomsan Electronic, Türkiye) was used to measure the changes in mass of the product, with the balance positioned within the drying chamber.

Calculation of Moisture Content, Drying Rate, and Dimensionless Mass Loss Ratio

To examine the thin-layer drying kinetics, the initial and final moisture content of the product to be dried are critical parameters. To determine the MC, MR and DR of the samples, Eq. 1, Eq. 2, and Eq. 3 were used respectively, which depends on factors such as the MC, PT, and drying conditions (temperature and pressure) of the product.

$$MC = \frac{M_t - M_e}{M_0} \times 100 \quad \dots (1)$$

$$MR = \frac{M_t - M_e}{M_0 - M_e} \quad \dots (2)$$

$$DR = \frac{MC_i - MC_{i+1}}{t_{i+1} - t_i} \times 100 \quad \dots (3)$$

In the equations, M₀= Initial MC, M_e= The equilibrium MC, M_t= The MC at time t, and M_{t+dt}= The MC at time t+dt.

Mathematical modeling of Thin Layer Drying Characteristics of Persimmon

The thin-layer drying kinetics of persimmons were analyzed using six widely used equations from the literature, as detailed in Table 1. The models were evaluated based on three criteria: R², χ², and RMSE.

Table 1 — Thin-Layer Drying Models

Model No	Model Name	Model Equation	Eq. No
1	Aghbaslo ¹⁸	$MR = \exp\left(-\frac{k_1 \times t}{1 + k_2 \times t}\right)$... (4)
2	Alibas ¹⁹	$MR = a \times \exp\left((-k \times t^n) + (b \times t)\right) + g$... (5)
3	Balbay&Sahin ²⁰	$MR = (1 - a) \times \exp(-k \times t^n) + b$... (6)
4	Improved ²¹ Midilli Kucuk	$MR = a \times \exp(-k_1 \times t^n) - \exp(-k_2 \times t^n) - b \times t^n$... (7)
5	Newton ²²	$MR = \exp(-k \times t)$... (8)
6	Page ²³	$MR = \exp(-k \times t^n)$... (9)

(n = Number of drying constants; a, b, c, g, k, k₁, k₂ = Drying constants; t = Time)

Table 2 — Evaluation criterion equations²⁵

Evaluation parameters	Evaluation criterion equations	Eq. No.
Reduced chi-square	$\chi^2 = \frac{\sum_{i=1}^N (MR_{exp,i} - MR_{pre,i})^2}{N - n}$... (10)
Root mean square error	$RMSE = \sqrt{\frac{\sum_{i=1}^N (MR_{pre,i} - MR_{exp,i})^2}{N}}$... (11)
Coefficient of determination	$R^2 = 1 - \frac{\sum_{i=1}^N (MR_{exp,i} - MR_{pre,i})^2}{\sum_{i=1}^N (MR_{exp,i} - MR_{avg})^2}$... (12)

(avg = average, exp = experimental; pre = predicted; N = Number of observation)

In the present study, nonlinear regression analysis was conducted to characterize the drying process and identify the most appropriate model. The models' fit to the experimental data was assessed using the criteria outlined in Table 2 (Eqs 10–12). The optimal model was determined as the one with the highest R² value and the lowest RMSE and χ^2 values based on the data from the drying experiments.²⁴

ANN Architecture

This research employed an MLP structure to model the FD process of persimmons across varying PTs and CPs. MLPs, known for their effectiveness in regression tasks, have been successfully applied to model drying processes.^{26–29} In this research, the feedforwardnet function in MATLAB R2024a was utilized to configure the MLP. The ANN architecture consists of an input layer, two hidden layers, and an output layer, illustrated in Fig. 1. The input layer incorporates features such as PT (I₁), CP (I₂), and DT (I₃), selected due to their substantial effect on the

drying kinetics observed in the experimental study. The hidden layers in this research include the first hidden layer with 5 neurons and the second hidden layer with 4 neurons. Determining the optimal number of hidden neurons usually involves experimental testing, and it has been demonstrated that two hidden layers with a sufficient number of neurons are capable of approximating complex functions in various applications, including drying kinetics.³⁰ Initial experiments in this study showed that two hidden layers provided satisfactory performance. The hidden layers utilize the tan-sigmoid activation function, which is the default in feed forward net. For the output layer, a linear activation function was employed, which is standard practice for regression problems due to its suitability for predicting continuous value ranges, such as drying parameters. The output layer includes the MR, MC, and DR parameters. The overall architecture of the ANN is illustrated in Fig. 1. The feed forward ANN was trained using the Levenberg–Marquardt

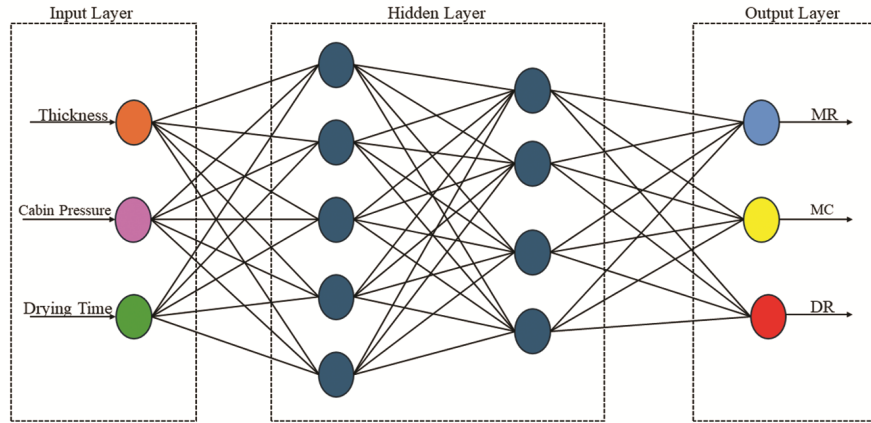


Fig. 1 — ANN architecture of persimmon FD process

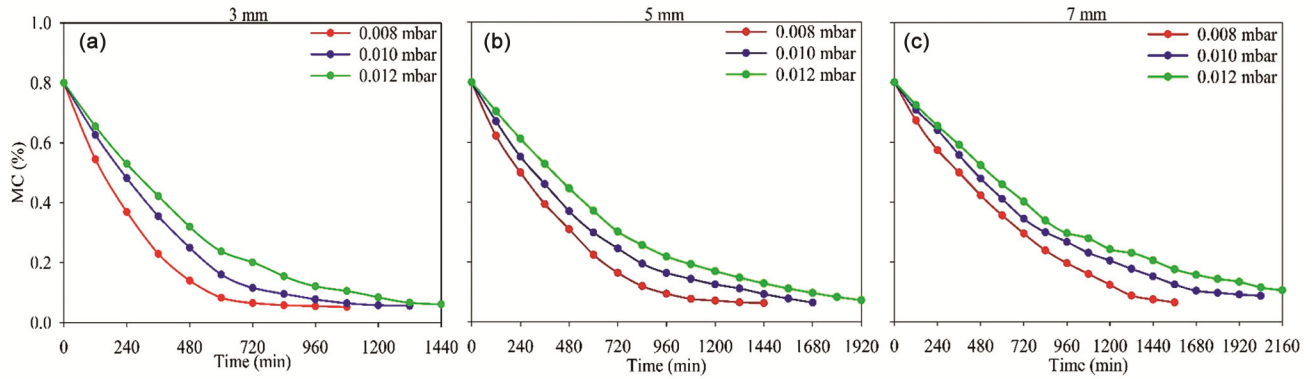


Fig. 2 — Change in the MC of persimmons based on PTs and CPs: (a) 3 mm, (b) 5 mm, and (c) 7 mm

algorithm, which is known for its efficiency in small-to medium-sized networks. A maximum of 1000 epochs was allowed, and to avoid overfitting, the training was terminated if the validation error failed to improve for 20 consecutive iterations ($max_fail = 20$).

The mathematical expressions that govern the behavior of the network are given in Eqs 13–16.

Weighted sum vector of first hidden layer (z^1):

$$z^1 = W^1 \times x + b^1 \quad \dots (13)$$

Weighted sum vector of second hidden layer (z^2):

$$z^2 = W^2 \times a^1 + b^2 \quad \dots (14)$$

Weighted sum vector of output layer (z^3):

$$z^3 = W^3 \times a^2 + b^3 \quad \dots (15)$$

Loss function (L):

$$L = \frac{1}{N} \sum \left(\|Y_{actual} - Y_{predict}\|^2 \right) \quad \dots (16)$$

Here, the weight matrices W^1 , W^2 , and W^3 , the input vector x , the bias vectors b^1 , b^2 and b^3 , the activation vectors a^1 and a^2 , the actual and predicted output vectors Y_{actual} and $Y_{predict}$, and the number of samples N are represented.

Results and Discussion

Impact of Drying Process on the MC and DR of Persimmons

The time-dependent changes in the MC of persimmons subjected to FD under varying PTs and CPs are depicted in Fig. 2. Experiments with PTs ranging from 3 mm to 7 mm and CPs from 0.008 mbar to 0.012 mbar demonstrated that the fastest drying occurred at a PT of 3 mm and a CP of 0.008 mbar, while the slowest drying was at a PT of 7 mm and a CP of 0.012 mbar. Comparing the final products based on their MC, the lowest MC of 5.2% was found in the product dried at 3 mm and 0.008 mbar, whereas the highest MC of 10.5% was observed in the product dried at 7 mm and 0.012 mbar. The findings indicate that increases in both CP and PT lead to longer DTs

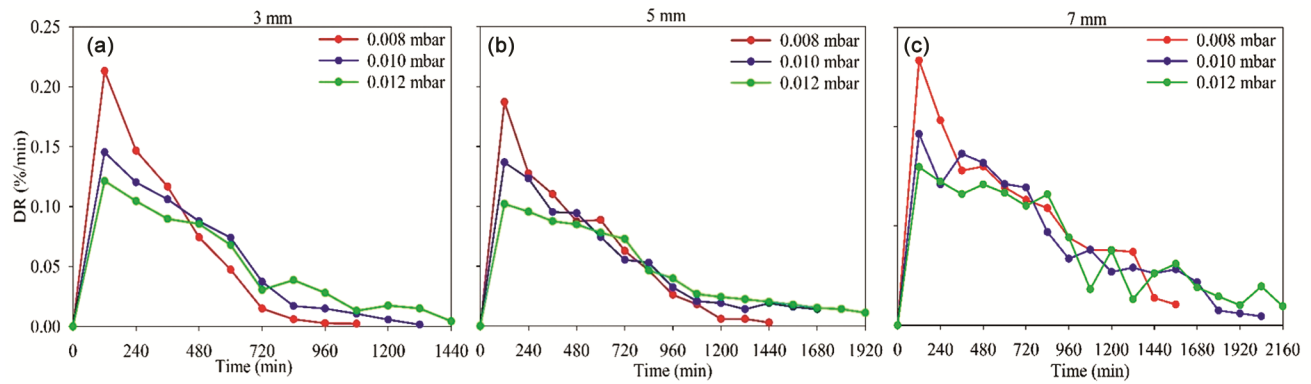


Fig. 3 — Change in the DR of persimmons based on PT and CP: (a) 3 mm, (b) 5 mm, and (c) 7 mm

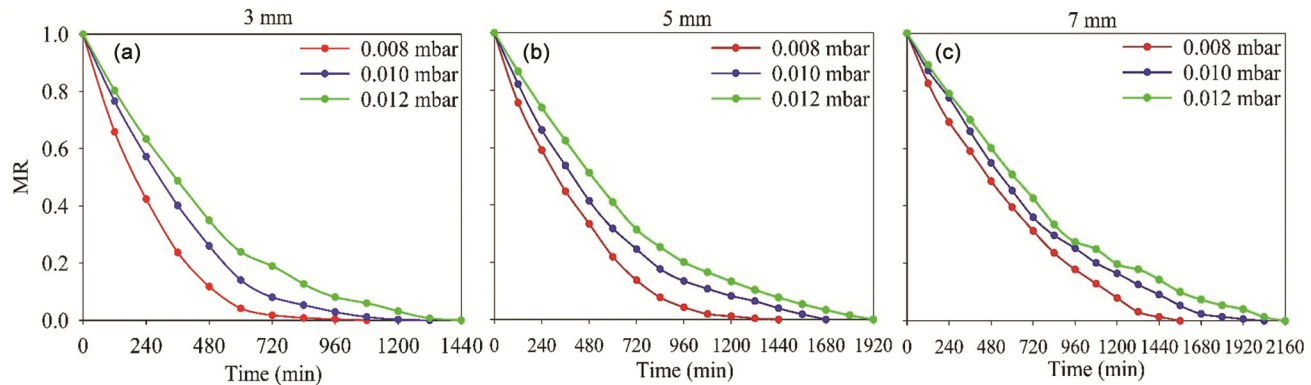


Fig. 4 — Change in the MR of persimmons based on PT and CP: (a) 3 mm, (b) 5 mm, and (c) 7 mm

and higher MC in the final product. As shown in Fig. 2, increasing the CP from 0.008 mbar to 0.012 mbar resulted in a prolonged DT. This observation aligns with previous studies.^{13,31} In this study, raising the CP from 0.008 mbar to 0.012 mbar significantly extended the DT for persimmons. Additionally, it was found that thicker products require more time for internal moisture to reach the surface and evaporate, resulting in longer drying durations. This trend, where DT increases with PT, is consistent with findings in other studies on FD and various drying techniques.^{32–35}

As illustrated in Fig. 3, the FD experiments performed at different PTs and CPs demonstrated that the DR generally decreases over time. The DR was found to be directly proportional to the MC, with the slope of the DR curves increasing as CP decreased. The maximum DR recorded during the FD of persimmons was 0.213%/min, achieved with a PT of 3 mm and a CP of 0.008 mbar. Additionally, it was evident that the DR was highest at the beginning of the process and decreased as the product's MC diminished. Initially, the rapid evaporation of free water on the product's surface, known as the constant

rate period, occurs quickly. After this phase, it was observed that DR decreased as MC decreased and drying occurred in the falling rate period. The FD experiments indicated that the DR of persimmons remained in the falling rate period, aligning with findings in the literature.^{36,37} Furthermore, it was observed that a decrease in CP led to an increase in the DR.

Mathematical Modeling Results of Thin-Layer Drying Characteristics of Persimmon

After the experimental studies, the FD kinetics of persimmons were analyzed using six different thin-layer drying models found in the literature and three different evaluation criteria. In this section, the MR-time curve graphs generated from the data obtained during the drying of persimmons are shown in Fig. 4, and the results of the evaluation criteria used to determine the model that best describes these curves are presented in Table 3.

Upon examining the results of the evaluation criteria at different PTs and CPs, it was determined that the models best describing the drying process for 3 mm thick persimmons were the Alibas model (0.008

Table 3 — Evaluation criterion results for FD of persimmon

PT ↓	M	CP →0.008 mbar			0.010 mbar			0.012 mbar		
		R ²	χ ²	RMSE	R ²	χ ²	RMSE	R ²	χ ²	RMSE
3 mm	1	0.8696	0.0222	0.1334	0.8439	0.0285	0.1540	0.7875	0.0416	0.1875
	2	0.9995	0.0001	0.0078	0.9989	0.0003	0.0129	0.9565	0.0117	0.0848
	3	0.9991	0.0002	0.0111	0.9988	0.0003	0.0131	0.9996	0.0001	0.0075
	4	0.9992	0.0002	0.0105	0.9989	0.0002	0.0128	0.9994	0.0002	0.0098
	5	0.9933	0.0010	0.0303	0.9897	0.0017	0.0395	0.9935	0.0012	0.0327
	6	0.9988	0.0002	0.0129	0.9471	0.0096	0.0896	0.9989	0.0002	0.0133
5 mm	1	0.8080	0.0343	0.1704	0.9996	0.0001	0.0078	0.7299	0.0539	0.2181
	2	0.9252	0.0184	0.1064	0.9995	0.0001	0.0088	0.9562	0.0109	0.0878
	3	0.9885	0.0025	0.0416	0.9997	0.0001	0.0077	0.9991	0.0002	0.0128
	4	0.9995	0.0001	0.0079	0.9965	0.0008	0.0237	0.9992	0.0002	0.0113
	5	0.9921	0.0013	0.0345	0.9965	0.0006	0.0236	0.9923	0.0014	0.0367
	6	0.9972	0.0005	0.0204	0.9994	0.0001	0.0101	0.9985	0.0003	0.0163
7 mm	1	0.9989	0.0002	0.0144	0.7370	0.0539	0.2189	0.9655	0.0074	0.0815
	2	0.9792	0.0062	0.0631	0.9611	0.0098	0.0842	0.9616	0.0101	0.0859
	3	0.9995	0.0001	0.0097	0.9989	0.0003	0.0140	0.9987	0.0003	0.0159
	4	0.9983	0.0005	0.0179	0.9995	0.0001	0.0099	0.9731	0.0070	0.0719
	5	0.9903	0.0020	0.0431	0.9898	0.0019	0.0430	0.9912	0.0018	0.0410
	6	0.9445	0.0124	0.1031	0.9971	0.0006	0.0230	0.9369	0.0136	0.1100

Table 4 — The most appropriate model and images from the FD experiments of persimmon

PT (mm)	CP (mbar)	Best model/Model equation
3	0.008	Alibas Model $MR = 1.3993 \times \exp(-0.0022 \times t^{1.0338}) - 0.0003 \times t - 0.3969$
	0.010	Improved Midilli-Kucuk Model $MR = 2.0016(0.0266 \times t^{0.5133}) - \exp(-0.1126 \times t^{0.5133}) - 0.1446 \times t^{0.5133}$
	0.012	Balbay & Sahin Model $MR = 1.0373 \times \exp(-0.0009 \times t^{1.1298}) - 0.0358$
5	0.008	Improved Midilli-Kucuk Model $MR = 2.0036(0.0148 \times t^{0.5829}) - \exp(-0.0444 \times t^{0.5829}) - 0.08 \times t^{0.5829}$
	0.010	Balbay & Sahin Model $MR = 1.0455 \times \exp(-0.0013 \times t^{1.049}) - 0.0382$
	0.012	Improved Midilli-Kucuk Model $MR = 1.9999(0.0214 \times t^{0.5029}) - \exp(-0.0891 \times t^{0.5029}) - 0.116 \times t^{0.5029}$
7	0.008	Balbay & Sahin Model $MR = 1.2895 \times \exp(-0.0017 \times t^{0.9325}) - 0.2836$
	0.010	Improved Midilli-Kucuk Model $MR = 1.9971(0.0151 \times t^{0.5437}) - \exp(-0.0572 \times t^{0.5437}) - 0.0815 \times t^{0.5437}$
	0.012	Balbay & Sahin Model $MR = 1.1762 \times \exp(-0.0011 \times t^{0.9832}) - 0.1460$

mbar), Improved Midilli-Kucuk model (0.010 mbar), and Balbay & Sahin model (0.012 mbar). For the drying process of 5 mm thick persimmons, Improved Midilli-Kucuk (0.008 mbar and 0.012 mbar) and Balbay & Sahin (0.010 mbar) models were found to be the best models that describe the process. Finally, when examining the results of the evaluation criteria for the drying process of 7 mm thick persimmons,

Balbay & Sahin (0.008 mbar and 0.012 mbar) and Improved Midilli-Kucuk (0.010 mbar) models were identified as the models that best describe the drying process.

Furthermore, Table 4 provides the equations of the most appropriate models for depicting the drying process of persimmons at different PTs and CPs. Images of the final dried products are shown in Fig. 5.

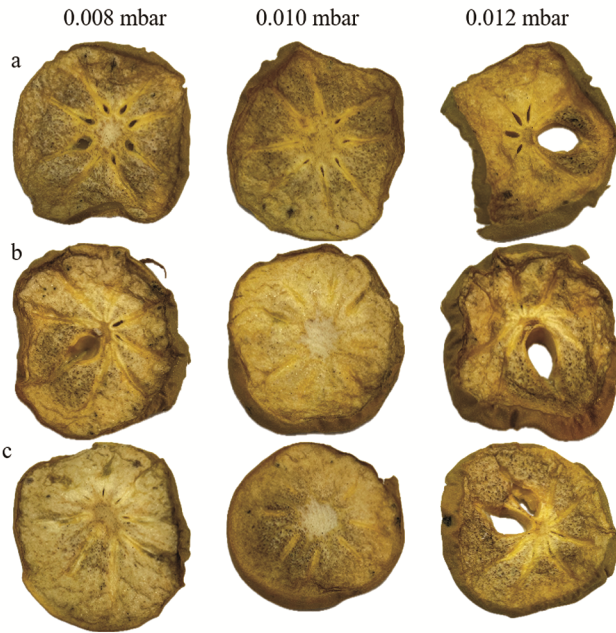


Fig. 5 — Images of FD samples of persimmon dried at different CP (mbar) with different PT: (a) 3 mm, (b) 5 mm, and (c) 7 mm

ANN Results for FD of Persimmons

In this study, ANN was employed to model the data collected during the FD process of persimmons. The ANN model, which consists of three inputs, three outputs, and two hidden layers, is analyzed and illustrated in Fig. 6. It was observed that the test performance value of the ANN and all performance value obtained from the analysis of all data were above 0.99. The closeness of the model results to 1 demonstrates the validity of using ANN for modeling the FD of persimmons. Similar high-performance results were also reported in recent studies involving ANN modeling of fruit drying kinetics³⁸⁻⁴⁰, further supporting the reliability of this approach.

In this section, the predicted and actual data obtained during the FD of persimmons are compared. The relationship between experimental values and the predicted data generated using ANN models are presented in Fig. 7. The graphs demonstrate that the ANN accurately predicted the MC, MR, and DR values for freeze-dried persimmons across different

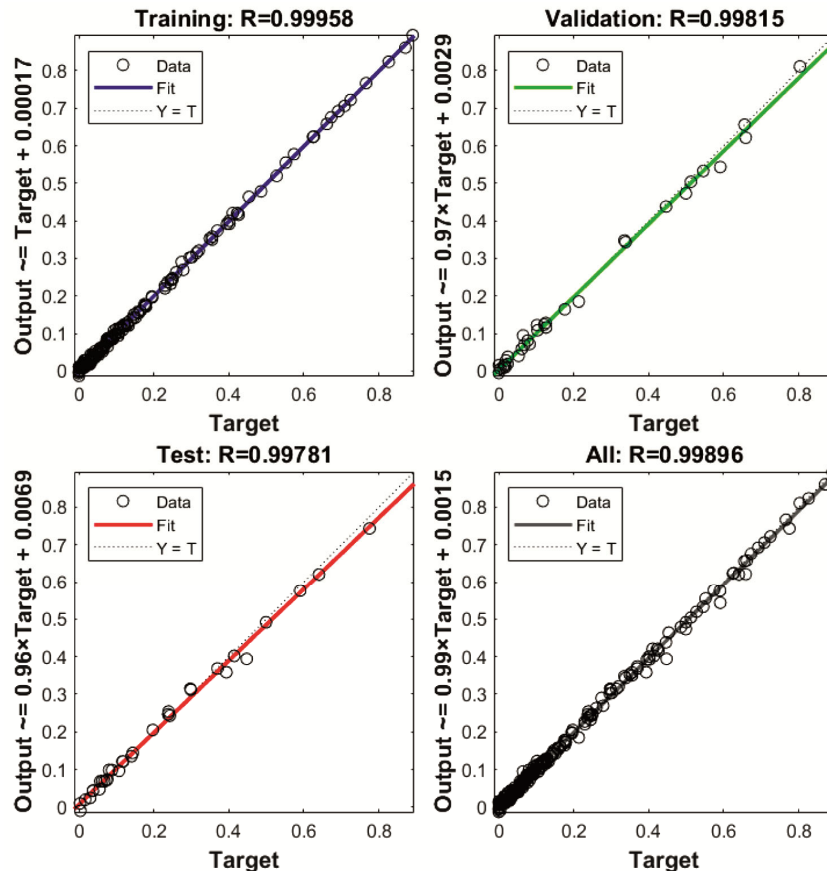


Fig. 6 — ANN results of freeze-dried persimmon

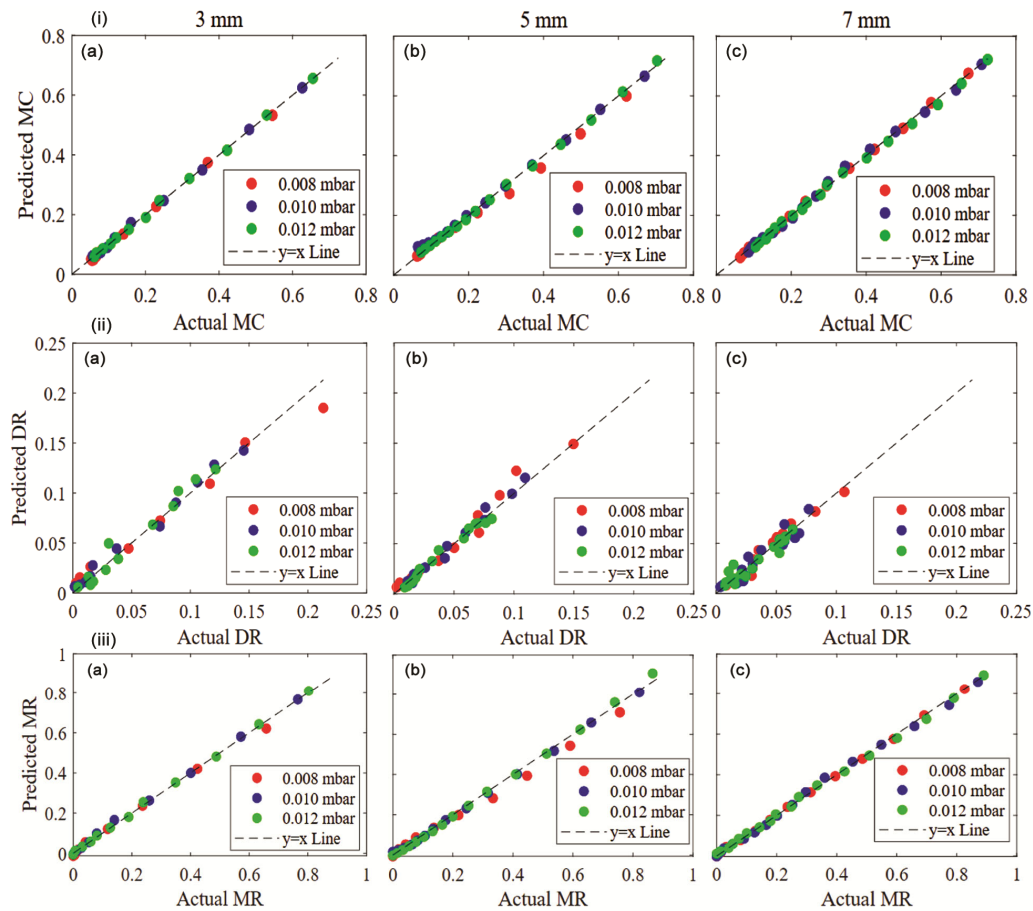


Fig. 7 — Experimental vs. ANN model predictions for persimmons: (i) MC, (ii) DR, and (iii) MR

PTs and CPs. These findings are in alignment with recent research where ANN models achieved high predictive accuracy in freeze-drying of fruit matrices under varying conditions.^{13,41}

As a result of this study, predictions of MC, MR, and DR values were obtained using ANNs, which demonstrated exceptional prediction capabilities and yielded results closely aligned with the experimental data. Incorporating recent advancements in ANN-assisted drying optimization, the current findings highlight the potential of ANN not only in predictive modeling but also in optimizing process parameters.^{42,43} It is anticipated that employing ANNs, combined with the adjustment of appropriate process conditions, could lead to savings in both time and cost.

Conclusions

In this study, the FD behavior of persimmons at varying PTs and CPs was successfully characterized using both mathematical models and ANN. The results revealed that decreasing CP and PT

significantly reduced DT, while the drying process predominantly occurred in the falling rate period. Among the models applied, the Alibas, Improved Midilli-Kucuk, and Balbay & Sahin models were most effective under different conditions. The ANN approach demonstrated a high prediction accuracy not only for the MR, but also for MC and DR, outperforming traditional modeling methods. A potential limitation of this study is that the ANN model was trained solely on experimentally obtained data without integration of external quality attributes. Future work could involve incorporating sensory or physicochemical quality data and expanding the dataset for better generalization. The modeling strategy applied here holds promise for optimizing drying parameters in industrial applications to enhance energy efficiency and product quality.

References

- Jain S, Ranganna G, Mohapatra S, Rathod M, Homeshvari, Kore D S, Saxena S & Anushi, A Comprehensive Review on Persimmon (*Diospyros kaki*): Botanical, horticultural, and

- varietal perspectives, *Int J Environ Clim*, **13** (2018) 4437–4457, doi: 10.9734/IJECC/2023/v13i113624.
- 2 Yılmaz A, Dođal, *Konveksiyonlu, Mikrodalga ve Kombine Mikrodalga-Konveksiyonlu Kurutma Yöntemlerinin Trabzon Hurmasının Biyoaktivitesi Üzerine Etkisi*, PhD Thesis, Uludağ University, Bursa, (2022).
 - 3 Tülek Y & Demiray E, Sıcak hava kurutma yönteminde farklı sıcaklık ve ön işlemlerin Trabzon hurmasının renk ve kuruma karakteristiklerine etkisi, *J Agric Sci*, **20** (2014) 27–37, <https://doi.org/10.15832/tbd.11768>.
 - 4 Wang D, Zhang M, Ju R, Mujumdar A S & Yu D, Novel drying techniques for controlling microbial contamination in fresh food: A review, *Dry Technol*, **41** (2023) 172–189, <https://doi.org/10.1080/07373937.2022.2080704>.
 - 5 Tan C H, Hii C L, Borompichaichartkul C, Phumsombat P, Kong I & Pui L P, Valorization of fruits, vegetables, and their by-products: Drying and bio-drying, *Dry Technol*, **40** (2022) 1514–1538, <https://doi.org/10.1080/07373937.2022.2068570>.
 - 6 Kalse S B, Jain S K, Swami S B, Panwar N L, Rajpurohit D, Wadhwan N & Bhatnagar A, A comprehensive review of mechanisms, heat transfer dynamics and the hybrid approach of refractance window™ drying, *Food Eng Rev*, **17** (2025) 319–343, <https://doi.org/10.1007/s12393-025-09399-5>.
 - 7 Ma Y, Yi J, Jin X, Li X, Feng S & Bi J, Freeze-Drying of fruits and vegetables in food industry: Effects on phytochemicals and bioactive properties attributes - A comprehensive review, *Food Rev Int*, **39** (2023) 6611–6629, <https://doi.org/10.1080/87559129.2022.2122992>.
 - 8 Silva-Espinoza M A, Ayed C, Foster T, Del Mar Camacho M & Martínez-Navarrete N, The impact of freeze-drying conditions on the physico-chemical properties and bioactive compounds of a freeze-dried orange puree, *Foods*, **9** (2020) 32, <https://doi.org/10.3390/foods9010032>.
 - 9 Egas-Astudillo L A, Martínez-Navarrete N & Camacho M M, Impact of biopolymers added to a grapefruit puree and freeze-drying shelf temperature on process time reduction and product quality, *Food Bioprod Process*, **120** (2020) 143–150, <https://doi.org/10.1016/j.fbp.2020.01.004>.
 - 10 Biernacka B, Dziki D, Rudy S, Krzykowski A, Polak R & Dziki L, Influence of pretreatments and freeze-drying conditions of strawberries on drying kinetics and physicochemical properties, *Processes*, **10** (2022) 1588, <https://doi.org/10.3390/pr10081588>.
 - 11 Selvi K Ç, Alkhaled A Y & Yıldız T, Application of artificial neural network for predicting the drying kinetics and chemical attributes of linden (*Tilia platyphyllos* Scop.) during the infrared drying process, *Processes*, **10** (2022) 2069, <https://doi.org/10.3390/pr10102069>.
 - 12 Zalpouri R, Singh M, Kaur P, Kaur A, Gaikwad K K & Singh A, Drying kinetics, physicochemical and thermal analysis of onion puree dried using a refractance window dryer, *Processes*, **11** (2023) 700, <https://doi.org/10.3390/pr11030700>.
 - 13 Topal M E, Şahin B & Vela S, Artificial neural network modeling techniques for drying kinetics of citrus medica fruit during the freeze-drying process, *Processes*, **12** (2024) 1362, <https://doi.org/10.3390/pr12071362>.
 - 14 Thuy N M, Van Hao H, Duong L T T, Giao T N, Minh V Q & Van T N, Foam-mat drying of lucuma powder: Mathematical and artificial modeling of drying kinetics, physicochemical and microstructural properties, *J Agric Food Res*, **19** (2025) 101656, <https://doi.org/10.1016/j.jafr.2025.101656>.
 - 15 Camilo M O, Carvalho R F, Costa A B S, Junior E F C, Costa A O S & Sousa R C, Drying kinetic for moisture content prediction of peels Tahiti lemon (*Citrus latifolia*): Approach by machine learning and optimization - genetic algorithms and nonlinear programming, *S Afr J Chem Eng*, **51** (2025) 136–152, <https://doi.org/10.1016/j.sajce.2024.10.005>.
 - 16 Azadbakht M, Aghili H, Ziaratban A & Torshizi M V, Application of artificial neural network method to exergy and energy analyses of fluidized bed dryer for potato cubes, *Energy*, **120** (2017) 947–958, <https://doi.org/10.1016/j.energy.2016.12.006>.
 - 17 Omari A, Behroozi-Khazaei N & Sharifian F, Drying kinetic and artificial neural network modeling of mushroom drying process in microwave-hot air dryer, *J Food Process Eng*, **41** (2018) 1–10, <https://doi.org/10.1111/jfpe.12849>.
 - 18 Aghbashlo M, Kianmehr M H, Khani S & Ghasemi M, Mathematical modelling of thin-layer drying of carrot, *Int Agrophys*, **23** (2009) 313–317.
 - 19 Alibaş I, Microwave drying of Grapevine (*Vitis vinifera* L.) leaves and determination of some quality parameters, *J Agric Sci*, **18** (2012) 43–53, <https://doi.org/10.1501/tarimbil.0000001191>.
 - 20 Balbay A & Şahin Ö, Microwave drying kinetics of a thin-layer liquorice root, *Dry Technol*, **30** (2012) 859–864, <https://doi.org/10.1080/07373937.2012.670682>.
 - 21 Midilli A & Kucuk H, Development of a new curve equation representing thin layer drying process, *Energy Sources A: Recovery Util Environ Eff*, **45** (2023) 9717–9730, <https://doi.org/10.1080/15567036.2023.2240740>.
 - 22 Topal M E & Şahin B, Freeze-Drying of tea leaves at different pressures: Effects on the thin-layer drying kinetics, water activity and color change, *J Anim Plant Sci*, **35** (2025) 689–700, <https://doi.org/10.36899/japs.2025.3.0058>.
 - 23 Okur O, Kucuk H & Midilli A, Triple-effect new generation drying technique, *Innov Food Sci Emerg Technol*, **89** (2023) 103489, <https://doi.org/10.1016/j.ifset.2023.103489>.
 - 24 Omolola A O, Jideani A I O & Kapila P F, Modeling microwave drying kinetics and moisture diffusivity of mabonde banana variety, *Int J Agric Biol Eng*, **7** (2014) 107–113, <https://doi.org/10.3965/j.ijabe.20140706.013>.
 - 25 Kucuk H, Midilli A, Kilic A & Dincer I, A review on thin-layer drying-curve equations, *Dry Technol*, **32** (2014) 757–773, <https://doi.org/10.1080/07373937.2013.873047>.
 - 26 Barriga R, Romero M, Nettleton D & Hassan H, Advanced data modeling for industrial drying machine energy optimization, *J Supercomput*, **78** (2022) 16820–16840, <https://doi.org/10.1007/s11227-022-04498-0>.
 - 27 Dash K, Bhagya Raj G & Gayary M, Application of neural networks in optimizing different food processes case study, mathematical and statistical applications in food engineering, *CRC Press*, **23** (2020) 346–362, <https://doi.org/10.1201/9780429436963-22>.
 - 28 Raj G V S B & Dash K K, Microencapsulation of dragon fruit peel extract by freeze-drying using hydrocolloids: optimization by hybrid artificial neural network and genetic algorithm, *Food Bioproc Tech*, **15** (2022) 2035–2049, <https://doi.org/10.1007/s11947-022-02867-4>.

- 29 Thapliyal D, Shrivastava R, Verros G D, Verma S, Arya R K, Sen P, Prajapati S C, Chahat & Gupta A, Modeling of triphenyl phosphate surfactant enhanced drying of polystyrene/p-xylene coatings using artificial neural network, *Processes*, **12** (2024) 260, <https://doi.org/10.3390/pr12020260>.
- 30 Torrecilla J S, Otero L & Sanz P D, Optimization of an artificial neural network for thermal/pressure food processing: Evaluation of training algorithms, *Comput Electron Agric*, **56** (2007) 101–110, <https://doi.org/10.1016/j.compag.2007.01.005>.
- 31 Kovacı T, Dikmen E and Şahin A Ş, Energy and exergy analysis of freeze-drying of mint leaves, *J Food Process Eng*, **43** (2020) 13528, <https://doi.org/10.1111/jfpe.13528>.
- 32 Demiray E, Yazar J G, Aktok Ö, Çulluk B, Çalışkan Koç G & Pandiselvam R, The effect of drying temperature and thickness on the drying kinetic, antioxidant activity, phenolic compounds, and color values of apple slices, *J Food Qual*, **2023** (2023) 7426793, <https://doi.org/10.1155/2023/7426793>.
- 33 Jiang N, Ma J, Ma R, Zhang Y, Chen P, Ren M & Wang C, Effect of slice thickness and hot-air temperature on the kinetics of hot-air drying of Crabapple slices, *Food Sci Technol*, **43** (2023), <https://doi.org/10.1590/fst.100422>.
- 34 Sadin R, Chegini G R & Sadin H, The effect of temperature and slice thickness on drying kinetics tomato in the infrared dryer, *Heat Mass Transf*, **50** (2014) 501–507, <https://doi.org/10.1007/s00231-013-1255-3>.
- 35 Hasibuan R, Haryanto B, Nafsun A I, Pramananda V, Siregar F F & Fazillah R, Drying of red ginger slices using tray dryer integrated with pyrolysis reactor as a heat source: Evaluation on the drying characteristics, red ginger quality, and drying kinetics, *Case Stud Chem Environ Eng*, **11** (2025) 101055, <https://doi.org/10.1016/j.cscee.2024.101055>.
- 36 Ismail N F, Mat Nawi H N & Zainuddin N, Mathematical modelling of drying kinetics of oven dried Hibiscus Sabdariffa seed, *J Phys Conf Ser*, **1349** (2019) 012144, <https://doi.org/10.1088/1742-6596/1349/1/012144>.
- 37 He C, Wang H, Yang Y, Huang Y, Zhang X, Arowo M, Ye J, Zhang N & Xiao M, Drying Behavior and Kinetics of Drying Process of Plant-Based Enteric Hard Capsules, *Pharmaceutics*, **13** (2021) 335, <https://doi.org/10.3390/pharmaceutics.13>.
- 38 Srivastava P K & Sit N, Mathematical and ANN modelling for convective drying of spanish cherry seeds: Bioactive degradation, energy efficiency, and mass transfer evaluation, *Food Biophys*, **20** (2025), <https://doi.org/10.1007/s11483-024-09898-8>.
- 39 Mahesh J S, Rengaraju B & Selvakumarasamy S, Effect of ANN and semi-empirical models on dried Annona muricata leaves, *Biomass Convers Biorefin*, **15** (2024) 6223–6235, <https://doi.org/10.1007/s13399-024-05546-w>.
- 40 Zalpouri R, Singh M, Kaur P, Singh S, Kumar S & Kaur A, Mathematical and artificial neural network modelling for refractance window drying kinetics of coriander (*Coriandrum sativum* L.) followed by the determination of energy consumption, mass transfer parameters and quality, *Biomass Convers Biorefin*, **15** (2023) 967–983, <https://doi.org/10.1007/s13399-023-05013-y>.
- 41 Sarkar T, Salauddin M, Hazra S K & Chakraborty R, Artificial neural network modelling approach of drying kinetics evolution for hot air oven, microwave, microwave convective and freeze dried pineapple, *SN Appl Sci*, **2** (2020), <https://doi.org/10.1007/s42452-020-03455-x>.
- 42 Ait Hmazi F, Bagar H, Madani A & Mrani I, A novel approach for modelling and predicting the drying kinetics of couscous grains using artificial neural networks, *J Food Compos Anal*, **132** (2024) 106301, <https://doi.org/10.1016/j.jfca.2024.106301>.
- 43 Subramanyam R & Narayanan M, Artificial neural network modeling for drying kinetics of paddy using a cabinet tray dryer, *Chem Ind Chem Eng Q*, **29** (2023) 87–98, <https://doi.org/10.2298/CICEQ220106017S>.